Kinetic Characterization of the Peptidase Activity of *Escherichia coli* Lon Reveals the Mechanistic Similarities in ATP-Dependent Hydrolysis of Peptide and Protein Substrates

Jennifer Thomas-Wohlever and Irene Lee*

Department of Chemistry, Case Western Reserve University, 10900 Euclid Avenue, Cleveland, Ohio 44106

Received January 14, 2002; Revised Manuscript Received May 30, 2002

ABSTRACT: Lon is an ATP-dependent protease that degrades unstructured proteins. In this study, we have examined the ATP dependency of *Escherichia coli* Lon catalyzing the hydrolysis of a defined fluorogenic peptide known as S3. Steady-state velocity analyses of S3 degradation in the presence of ATP, or the nonhydrolyzable ATP analogue AMPPNP, indicate a sequential mechanism, and the k_{cat} of the reaction was 7-fold higher in the presence of ATP. Comparing the pre-steady-state time courses of the ATP- versus AMPPNP-mediated S3 hydrolysis reveals that ATP hydrolysis accelerates a slow step before the chemical cleavage of peptide. Product inhibition studies indicate that ADP is competitive versus ATP but noncompetitive versus the S3 substrate. In the absence of S3, Lon exhibits a 10−20-fold higher affinity for ADP than ATP. However the S3 substrate weakens the affinity of Lon for ADP by 7−19-fold, indicating that this peptide also promotes ADP/ATP exchange in Lon similar to that observed with protein substrates. The hydrolyzed peptide product, Pd1, exhibited noncompetitive inhibition versus both ATP and S3 substrates. Together with the small change in the K_i of Pd1 at increasing S3 concentrations, the Pd1 inhibition data support the existence of an isomechanism in Lon catalyzing the hydrolysis of S3 in the presence of ATP or AMPPNP. Upon the basis of the collected data, an extended kinetic mechanism is proposed for the ATP-dependent peptidase mechanism of Lon.

Lon protease, also known as protease La, belongs to a class of ATP-dependent serine protease functioning to degrade misfolded/nonsense proteins as well as certain short-lived regulatory proteins (for reviews, *1*−*3*). Lon was first isolated as the translational product of the *lon* (*capR*) gene in *Escherichia coli* (*E. coli*, *4*). Homologues of *lon* have since been found in the mitochondria of eukaryotic cells (*5*−*8*). In *E. coli*, Lon functions as a homotetramer with each subunit having a molecular weight of 88 kDa. Each monomeric subunit contains an ATPase and a peptidase site. The existence of an allosteric protein-binding site that activates the ATPase activity of Lon has also been implicated (*2*), but the location of this site in the protease has yet to be determined. Optimal polypeptide degradation activity of Lon is maintained by the kinetic coordination of the ATPase, the peptidase, and the putative allosteric protein binding sites (*3*).

In vivo, Lon degrades polypeptides with concomitant hydrolysis of ATP to yield small peptide fragments that are 5−10 amino acids long and ADP, which is a potent product inhibitor (*3*, *9*, *10*). Lon displays broad primary sequence specificity in degrading polypeptides. Analysis of the Lon cleavage sites in protein substrates reveals that Lon prefers to cleave after hydrophobic residues, but numerous exceptions to this rule have been detected in the Lon cleavage profiles of protein substrates (*3*, *11*−*13*). Lon also hydrolyzes certain hydrophobic methoxynaphthylamide tetrapeptides containing only one Lon cleavage site. Compared to protein substrates, the specificity constants (V/K_m) for the tetrapeptides are 1000-fold lower, and the catalytic efficiency of tetrapeptide cleavage is affected by altering the amino acids distal from the scissile bond (*14*). Therefore, the peptide substrate specificity is not strictly determined by the amino acids at the site of cleavage.

Since ATP is the physiological activator of Lon protease, an understanding of the kinetic coordination of the ATPase and the peptidase activity of Lon is important for understanding the mechanism of this enzyme. For example, an interesting paradox is that protein substrates stimulate (*10*, *15*, *16*) while methoxynaphthylamide tetrapeptides inhibit the ATPase activity of Lon (*14*). It is proposed that only the former substrates interact with Lon allosterically to stimulate ATP hydrolysis by promoting ADP release from the enzyme, which has been assumed to be the rate-limiting step of the reaction (*3*). This model predicts that peptide cleavage occurs before ATP hydrolysis, and the catalytic turnover of peptide cleavage is dependent on the substrate's ability to promote ADP release from the enzyme. Furthermore, because the nonhydrolyzable ATP analogues such as AMPPNP[1] support peptide cleavage in unstructured substrates without generating ADP, it is proposed that nonhydrolyzable ATP analogues bind and lock Lon in an active conformation to carry out peptide bond cleavage (*3*, *12*). According to this hypothesis, one anticipates that the nonhydrolyzable ATP analogues are more effective than ATP in supporting the degradation of unstructured polypeptides by Lon, as no ADP is generated

* Corresponding author. Phone: 216-368-6001. Fax: 216-368-3006. E-mail: ixl13@po.cwru.edu.

10.1021/bi0255470 CCC: $22.00 © 2002 American Chemical Society
Published on Web 07/02/2002

to inhibit Lon. On the contrary, the catalytic efficiencies of ATP-mediated unfolded polypeptide cleavage are higher, though in some instances comparable to, those values determined for the AMPPNP-mediated peptidase reactions (*3*, *12*). Since ADP release does not participate in the reaction pathway of AMPPNP-mediated peptide hydrolysis, we question how ATP hydrolysis contributes to the catalytic efficiency of unstructured peptide cleavage and the location of the rate-limiting step in the AMPPNP-mediated peptidase reaction.

Using fluorescence resonance energy transfer techniques, we have shown that ATP is more effective than AMPPNP in mediating the cleavage of an unstructured 11 amino acids long fluorescent peptide (S1, Figure 1, also known as FRETN 89−98 in our previous study, *17*) containing a unique Lon cleavage site. The sequence of this peptide was designed to mimic the truncated carboxyl terminus of the λ N protein, which is a physiological substrate of *E. coli* Lon (*12*). The k_{cat}/K_m values of the two substrates are comparable, and Lon cleaved both substrates at the same scissile bond between a Cys and Ser residue. The intrinsic ATPase activity of Lon was also stimulated by the synthetic peptide S1 as well as by the native protein substrate λN (*12*, *17*). In this study, we compared the kinetic parameters of ATP- versus AMP-PNP-mediated S1 cleavage to quantify the contribution of ATP hydrolysis toward peptide cleavage. We also examined the kinetic mechanism of ADP and hydrolyzed peptide product inhibition to identify different enzyme forms existing in the peptidase pathway of Lon under steady-state conditions. The elucidation of a minimal kinetic mechanism in this study allows for the construction of a working model to account for the functional consequences of the kinetic coordination of ATPase and peptidase activity in Lon catalysis.

EXPERIMENTAL PROCEDURES

Materials. Fmoc-protected amino acids, Boc-Abz, and Fmoc-protected Lys Wang resin and HBTU were purchased from Advanced ChemTech and NovaBiochem. HATU was purchased from PerSeptive Biosystem. All solvents and reagents used for peptide synthesis were purchased from Acros, Aldrich, and Fisher. ATP, AMPPNP, and ADP were purchased from Sigma. Tris buffer, cell culture media, IPTG, and chromatography media were purchased from Fisher and Sigma.

General Methods. The peptide substrates S1 and S2 and the peptide product Pd1 were synthesized using Fmoc solid-phase synthesis methodologies (*18*), and *E. coli* Lon was

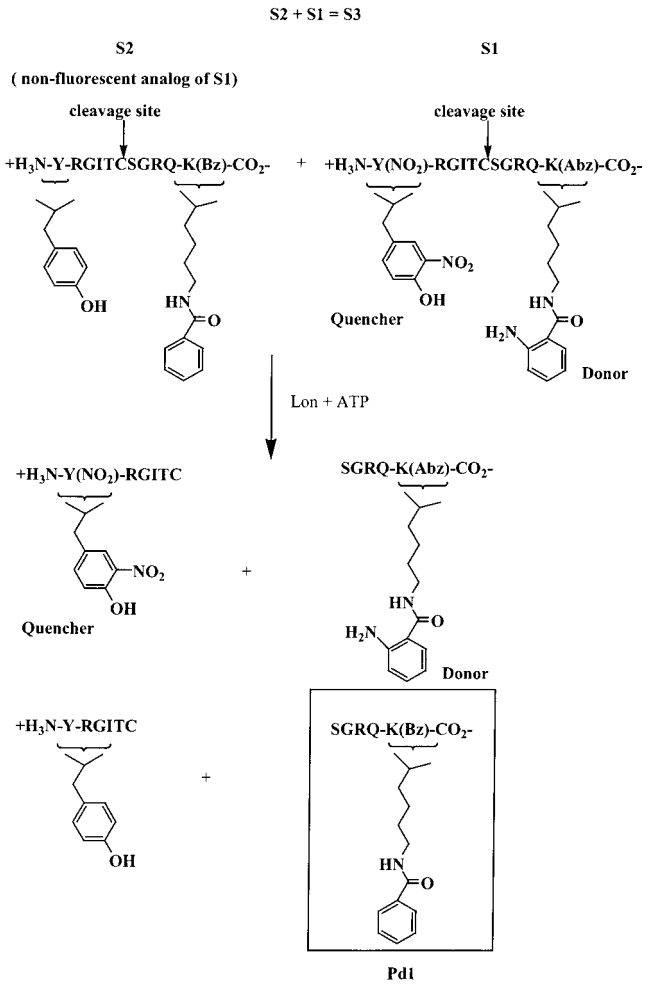

FIGURE 1: ATP-dependent peptide cleavage by *E. coli* Lon. S1 is the fluorogenic substrate, and S2 is the nonfluorescent analogue of S1. The S3 peptide substrate used in this study contains 5% S1 and 95% S2. After incubation with Lon and ATP, the substrate is hydrolyzed into the products shown, including Pd1 (in the box).

purified and quantitated as previously described (*3*). In brief, *E. coli* cells hosting the Lon expression vector pSG11 (*3*) were grown in superbroth (SB, per L: 30 g bactotryptone, 20 g yeast extract, 10 g MOPS, pH 7, 100 μg/mL amp) at 37 °C and induced with 1 mM IPTG at $OD_{600} = 1.5$ for two additional hours. Cell lysate was loaded onto a phosphocellulose column preequilibrated with 50 mM KPi, pH 7, 2 mM DTT, and 20% glycerol and then eluted with a linear gradient of KPi buffer (0.1−0.5 M KPi, pH 7, 2 mM DTT, 20% glycerol). Lon positive fractions (eluted between 0.25 and 0.4 M KPi) were pooled, concentrated by an amicon concentrator and then dialyzed into 50 mM Tris, pH 8.0, 2 mM DTT, and 20% glycerol. The dialyzed protein was loaded onto a DE 52 column equilibrated with the same Tris buffer. The resulting column was eluted with a linear KPi gradient (70−100 mM KPi, pH 7, 2 mM DTT, 20% glycerol). Lon was further eluted with 0.1 M KPi until all the protein was removed from the column, as judged by 12% SDS−PAGE. The Lon positive fractions were pooled and then precipitated with 80% ammonium sulfate (w/v). The precipitate was recovered by centrifugation and then dissolved in minimum amount of 75 mM KPi, pH 7, 2 mM DTT, 20% glycerol prior to purification by a Superose 6 (Pharmacia) gel filtration column equilibrated with the same

[1] Abbreviations: AMPPNP, adenylyl 5-imidodiphosphate; DTT, dithiothreitol; Fmoc, 9-fluorenylmethoxycarbonyl; Boc, butoxycarbonyl; HATU, 2-(1*H*-9-azabenzotriazole-1-yl)-1,1,3,3-tetramethyluronium hexafluorophosphate; HBTU, *O*-benzotriazole-*N*,*N*,*N*′,*N*′-tetramethyluronium hexafluorophosphate; FRET, fluorescence resonance energy transfer; Abz, anthranilamide; Tris, 2-amino-2-(hydroxymethyl)-1,3-propanediol; amp, ampicillin; KPi, potassium phosphate; λ N, also known as the λ N protein, a λ phage protein that allows *E. coli* RNA polymerase to transcribe through termination signals in the early operons of the phage; S1, also known as the FRETN 89−98 peptide in our previous study, contains amino acid residues 89−98 of the λ N protein; S2, a nonfluorescent analogue of S1 that is cleaved by Lon identically as S1; S3, a mixed peptide substrate containing 5% S1 and 95% S2 designed to overcome the inner filter effect observed in S1; Pd1, the hydrolyzed product of S2 containing the last five amino acids from the carboxyl terminal of S2.

phosphate buffer. Lon recovered from gel filtration chromatography was concentrated and stored in aliquots at −80 °C. The removal of ADP from Lon was monitored by the shift in the maximum absorption of the protein from 275 to 280 nm in the UV spectra of the protease. Bradford assays were used to quantify Lon monomer concentrations using Lon monomer standards. The Lon monomer standards were prepared from diluted stocks of a Lon sample, whose concentration was determined by quantitative amino acid analysis.

Steady-State Velocity and Product Inhibition Studies. Steady-state velocity data were collected on a Fluoromax 3 spectrofluorimeter (Horiba Group) equipped with a temperature-regulated cell holder connected to circulating water bath to maintain a constant temperature of 37 °C. All assays were performed in microcuvettes (Hellma) with a 3-mm path length. A typical assay contained 50 mM Tris HCl, pH 8.1, 2 mM magnesium acetate, 2 mM DTT, 125 nM *E. coli* Lon monomer, and varying concentrations of nucleotide (ATP or AMPPNP) or peptide substrate (S3) in the absence or presence of ADP or the hydrolyzed peptide product (Pd1). The enzyme was preincubated with peptide substrate in the absence or presence of inhibitor in the reaction buffer at 37 °C for 1 min prior to initiation of the reaction by ATP. The progress of the peptide cleavage reaction was monitored by the increase in fluorescence (excitation 320 nm, emission 420 nm). The degree of peptide hydrolysis was calibrated by determining the maximum fluorescence generated per micromolar peptide due to complete digestion by trypsin under identical reaction conditions.

Data Processing. The steady-state rates were determined from tangents to the linear steady-state portions of the reaction time courses using the computer program KaleidaGraph (Synergy, Inc.). All experiments were performed in triplicate, and the standard deviation among the values was within 10%, except for assays performed at very high inhibitor or low substrate concentrations, in which case the standard deviation was within 20%. The appropriate equations (*19*) were fit to the experimental data using the software program Enzfitter (Biosoft). The sigmoidal velocity versus substrate concentration curve for S3 cleavage was fit by eq 1. The general bireactant eq 2 was fit to the steady-state velocity data for peptide cleavage at varying ATP and S3 concentrations. The product inhibition data were fit by eq 3 for noncompetitive inhibition and by eq 4 for competitive inhibition. The intrinsic dissociation constant and the Michaelis constant of A were deduced from K_{ia}' and K_a', respectively, using eq 5:

$$v = VA^n/(A^n + K_a') \quad (1)$$

$$v = VA^nB/(K_{ia}'K_b + K_a'B + K_bA^n + AB) \quad (2)$$

$$v = VA^n/(K_a'[1 + I/K_{is}] + A^n[1 + I/K_{ii}]) \quad (3)$$

$$v = VA^n/(K_a'[1 + I/K_{is}] + A^n) \quad (4)$$

$$\log K = (\log K')/n \quad (5)$$

In eqs 1−4, v is the steady-state velocity, V is the maximum velocity, A is the S3 peptide substrate concentration, B is the ATP concentration, n is the Hill coefficient, and K_b is the Michaelis constant for ATP. I is the inhibitor concentration, and K_{is} and K_{ii} are the inhibition constants at low and high concentrations of the varying substrate, respectively.

Pre-Steady-State Time Courses of S1 Cleavage by Fluorescent Stopped Flow. Pre-steady-state experiments were performed on a KinTek Stopped Flow controlled by the data collection software Stop Flow v7.50 beta. The sample syringes were maintained at 37 °C by a circulating water bath. Syringe A contained 10 μM Lon monomer, 1.6 mM (30% S1 + 70% S2) peptide substrate, and the typical reaction components, including 5 mM $Mg(OAc)_2$, 2 mM DTT, and 50 mM Tris pH 8.1. Syringe B contained 2 mM ATP or AMPPNP, 5 mM $Mg(OAc)_2$, 2 mM DTT, and 50 mM Tris pH 8.1. Peptide cleavage was detected by an increase in fluorescence (excitation 320 nm, emission 420 nm) following rapid mixing of syringe contents in the sample cell. Data shown are the result of normalizing the baseline fluorescence to zero, and averaging at least six traces. The lag equation (*20*) was fit to the averaged time courses:

$$F = v_f t - (v_f - v_i)/k\{1 - \exp(-kt)\} \quad (6)$$

where F is the relative fluorescent intensity, v_f is the final velocity, v_i is the initial velocity, t is time in second, and k is the apparent lag rate of the time courses.

RESULTS

Utilization of a Mixed Peptide Substrate to Monitor the Peptidase Activity of Lon. We previously developed an 11-amino-acid fluorogenic peptide as a substrate for Lon. Cleavage of this peptide, designated as S1, was accurately monitored by the increase in fluorescence that accompanied the separation of an anthranilamide group from nitrotyrosine upon cleavage by Lon. The maximum fluorescence generated from complete cleavage of S1 by trypsin is linear up to only 160 μM due to interference by the inner filter effect (*17*). Therefore, to expand the utility of S1 as Lon substrate above 160 μM, we utilized a mixed peptide substrate composed of S1 and S2 (Figure 1) to monitor the time courses of peptide cleavage by Lon. We synthesized S2, a nonfluorescent analogue of S1, by replacing the fluorophore anthranilamide with benzoic acid amide and the nitrotyrosine quencher with tyrosine and digested various concentrations of a peptide mixture (S3) containing 5% S1 and 95% S2 with trypsin. The fluorescence signal generated from complete trypsin digestion of peptide S3 is linear up to 800 μM total peptide concentration (data not shown) and suggest that S2 can be used as a fluorescently silent cosubstrate in the fluorescence peptidase assay.

A lag phase was detected prior to attainment of a steady-state rate in all time courses generated under excess substrate over enzyme conditions regardless of whether S1 or S3 was used as the substrate. Representative time courses obtained by Lon cleaving 50 μM of S3 in the presence of ATP as well as in the presence of ATP and ADP are provided in Figure 2. The initial lag phase was not dependent on preincubation with peptide since a similar lag was observed when Lon was added to the reaction last. However, preincubation of Lon with ATP prior to addition of the peptide substrate increases the duration of the lag phase.

Despite the presence of the lag, steady-state rates were measured from the tangents of the time courses as described under data processing in the Experimental Section. The

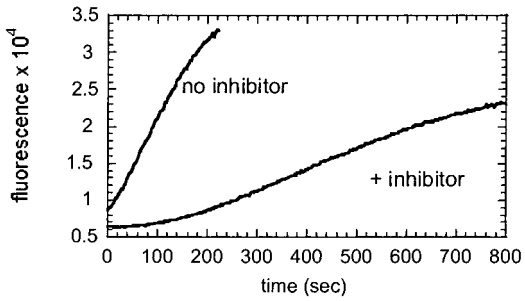

FIGURE 2: Measurement of the steady-state velocity from the progress curve of fluorescence change associated with S3 cleavage by Lon. *E. coli* Lon (125 nM) was incubated with 50 μM S3 in the absence and presence of ADP as described in experimental prior to addition of ATP. The time course of each reaction is monitored by the increase in fluorescence at excitation 320 nm and emission at 420 nm. The steady-state rate of fluorescence change is obtained from the tangent of the steady-state phase of the time course. The rate of peptide hydrolysis is calculated by dividing the rate of fluorescence changes by the amount of fluorescence generated from tryptic digestion of 1 μM of peptide as described by Lee and Berdis (*17*).

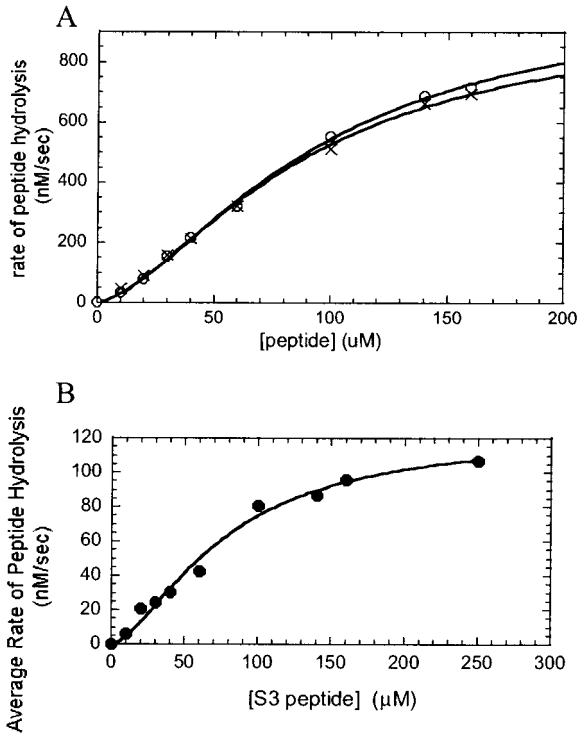

FIGURE 3: Velocity curve of S1 or S3 cleavage by *E. coli* Lon in the presence of 500 μM ATP or AMPPNP. (A) The rates of peptide cleavage were determined at 125 nM of *E. coli* Lon monomer and varying concentrations of S1 (×) or S3 (○) in the presence of 500 μM ATP. Data points are experimental, and the lines are derived from a fit of the data using eq 1. (B) The rates of S3 cleavage were determined as described in panel A, except that 500 μM of AMPPNP was used in place of ATP.

steady-state rates of peptide cleavage in the presence of either 500 μM ATP or AMPPNP were plotted against the corresponding peptide concentrations as depicted in panels A and B, respectively, of Figure 3. The kinetic parameters associated with S3 cleavage by Lon in the presence of ATP agree closely with the parameters determined using S1 using the same enzyme preparation (Table 1). To verify the utility of our assay system, we independently monitored the time courses of S2 (the 95% cosubstrate of S3) cleavage by Lon using reverse-phase HPLC. The kinetic parameters determined for S2 cleavage in the presence of 500 μM ATP were identical to those determined in the fluorescence peptidase assay using either S1 or S3 as substrate (Supporting Information).

Table 1: Steady-State Kinetic Parameters of ATP- versus AMPPNP-Mediated Peptide Cleavage[a]

parameters	500 μM ATP ± SE S3 substrate	500 μM ATP ± SE S1 substrate[b]	500 μM AMPPNP ± SE
K_a[c] (μM)	85 ± 4	84 ± 5	77 ± 7
n	1.60 ± 0.05	1.56 ± 0.03	1.6 ± 0.2
K_b (μM)	7.2 ± 1.1[e]		10.0 ± 1.0[e]
V_{max} (nM/s)	963 ± 28[d] (589 ± 24)[e]	834 ± 10	125 ± 6[d] (50 ± 1)[e]
K_a' (μM)	1200 ± 120[e]	1000 ± 100	760 ± 60[e]
K_{ia}' (μM)	660 ± 300[e]		750 ± 150[e]
k_{cat}[f]	7.7/s (4.7/s)[e]	6.7/s	1/s

[a] Subscript a denotes S3 or S1 peptide substrate, whereas b is either ATP or AMPPNP. [b] The kinetic parameters for S1 cleavage were obtained by fitting eq 1 to the data obtained for 10, 20, 30, 40, 60, 100, 140, and 160 μM peptide cleavage in the presence of 500 μM ATP to yield yield K_a'. The K_a values were then obtained from the K_a' and the n values using eq 5. [c] These values were determined by first fitting eq 2 to the rate data to yield K_a'. The K_a values were then obtained from the K_a' and the n values using eq 5. [d] These values were obtained by fitting eq 1 to the data obtained at 10−160 μM peptide substrate concentrations. [e] These values were obtained by fitting eq 2 to the data at 50, 100, 150, and 200 μM peptide and at 5, 10, 50, 75, 150, and 250 μM ATP. [f] These values were obtained by dividing V_{max} by total Lon monomer concentration, which is 125 nM.

Steady-State Velocity Studies of ATP- and AMPPNP-Mediated S1 Cleavage in the Absence of Added Inhibitors. The steady-state velocities of S3 cleavage were monitored at varying concentrations of S3 while maintaining the concentration of either ATP or AMPPNP constant. Alternatively, the velocities were monitored at various nucleotide levels but at a fixed peptide concentration. The double reciprocal plot of the initial velocity data intersects to the left of the ordinate in the ATP- as well as in the AMPPNP-dependent reactions (plots not shown), suggesting a sequential kinetic mechanism for peptide cleavage. Equation 2 was fit directly to the velocity data and the resulting kinetic parameters are summarized in Table 1. Both the ATP- and AMPPNP-mediated S3 peptidase reactions exhibit sigmoidal kinetics with nearly identical K_a, K_b and Hill coefficient values. However, the k_{cat} of ATP-mediated S3 hydrolysis is 7.7/s, which is 7-fold higher than that of AMPPNP.

Pre-Steady-State Time Courses of ATP- and AMPPNP-Mediated S1 Cleavage at Saturating Substrate Conditions. Nucleotide-free *E. coli* Lon preincubated with 10× K_m the amount of S3 (containing 30% S1 and 70% S2 in the pre-steady-state study) was rapidly mixed with a saturating concentration of ATP or AMPPNP (1 mM) in a stopped flow apparatus. An increase in fluorescence was detected upon exciting the reaction at 320 nm. As shown in Figure 4, a lag phase was detected in the beginning of the time course using 5 μM *E. coli* Lon monomer (final concentration) in the reaction. The time course represents an average of at least six traces. The kinetic parameters obtained by fitting eq 6 to the time courses as described in methods are summarized in Table 2, which shows that values obtained for the AMPPNP-mediated S1 cleavage are lower than those for the

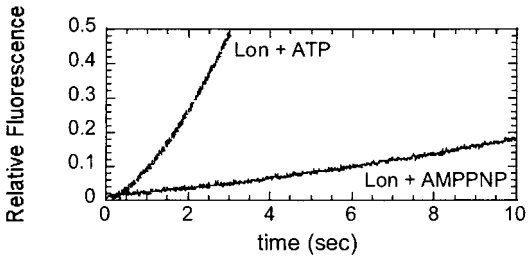

FIGURE 4: Pre-steady-state time courses of S3 cleavage at saturating substrate conditions. The ATP- and AMPPNP-dependent cleavage of 800 μM of S3 (30% S1 and 70% S2) by 5 μM Lon monomer in the presence of 1 mM ATP or AMPPNP (all reagents are reported as final concentrations) was monitored by fluorescence stopped flow at 37 °C. The time course for the ATP-dependent reaction was an average of 10 traces, whereas the time course for the AMPPNP-dependent reaction was an average of 6 traces. The averaged time courses were fit by eq 6 to yield the kinetic parameters summarized in Table 2.

Table 2: Pre-Steady-State Kinetic Parameters for the ATP- versus AMPPNP-Mediated Peptide Cleavage[a]

parameters	ATP	AMPPNP
v_i (Δ fluorescence/s)	0.024 ± 0.002	0.0094 ± 0.0006
v_f (Δ fluorescence/s)	0.25[b]	0.027 ± 0.003
k (s^{-1})	0.76 ± 0.03	0.12 ± 0.04

[a] The parameters are obtained by fitting the pre-steady-state time course for S3 cleavage in the presence of ATP or AMPPNP to eq 6. [b] The standard error of the fit is less than 1%.

Table 3: ADP Inhibition Analyses of ATP-Dependent Peptide Cleavage by *E. coli* Lon

varied substrate	fixed substrate	inhibitor	pattern	$K_{is} \pm$ SE (μM)	$K_{ii} \pm$ SE (μM)
ATP	80 μM S3	ADP	C	0.8 ± 0.2	
S3	10 μM ATP	ADP	NC	$1.0 \pm 0.1(0.3)$[a]	7 ± 1
S3	100 μM ATP	ADP	NC	$10 \pm 1(0.5)$[a]	50 ± 9
S3	500 μM ATP	ADP	NC	$52 \pm 1(0.7)$[a]	500 ± 22

[a] These values correspond to the intrinsic K_i for ADP calculated from the equation $K_{i,app} = K_i(1 + ATP/K_b)$.

ATP-mediated reaction. Table 2 also shows that while the initial rates (v_i) of the two nucleotide-dependent reactions differ by 2.6-fold, their lag rate constants and their final velocities (v_f) differ from one another by 6−10-fold.

ADP Inhibition Studies. The steady-state velocities of ADP inhibiting S3 hydrolysis by Lon were determined at a constant level of one substrate and at varying concentrations of the other substrate at several fixed levels of ADP. The respective inhibition constants determined are summarized in Table 3. When the concentration of ADP was varied against ATP at 80 μM (K_a level) S3, the steady-state velocity data were best fit by the equation for a competitive inhibition (eq 4) yielding a K_{is} of 0.8 μM for ADP. When the concentration of ADP was varied against S3 at 10 μM (K_b), 100 μM (10 × K_b), or 500 μM (50 × K_b) ATP, the velocity data were best fit by eq 3 that describes a noncompetitive inhibition pattern. At each fixed ATP concentration, the K_{is} of ADP is lower than the K_{ii} value. Comparison of the intrinsic K_{is} obtained for ADP (0.3−0.7 μM, Table 3) with the K_b of ATP (7.2 μM, Table 1) suggests that ADP binds to Lon with higher affinity than ATP. Comparing the respective K_{is} or K_{ii} values determined at the three different ATP concentrations versus varying peptide also indicate that the apparent inhibition constant for ADP increases with increasing ATP, which is consistent with both nucleotides competing for the same site in Lon.

Table 4: Hydrolyzed Peptide Product Inhibition Studies of ATP-Dependent Peptide Cleavage by *E. coli* Lon Protease

varied substrate	fixed substrate	inhibitor	pattern	$K_{is} \pm$ SE (μM)	$K_{ii} \pm$ SE (μM)
S3	500 μM ATP	Pd1	NC	270 ± 5	200 ± 5
S3	500 μM AMPPNP	Pd1	NC	300 ± 60	200 ± 16
ATP	80 μM S3	Pd1	NC	270 ± 70	350 ± 30
ATP	600 μM S3	Pd1	NC	450 ± 20	450 ± 3

Peptide Production Inhibition Studies. The inhibitory effects of one of the hydrolyzed peptide products containing the last five residues of S2 (Figure 1, Pd1) on the peptidase activity of Lon were examined. The steady-state velocity data were best fit by the noncompetitive inhibition eq 3 when the concentration of Pd1 was varied against the concentrations of S3 at 500 μM ATP or AMPPNP. The inhibition constants deduced from the fits are summarized in Table 4. As shown in Table 4, the respective K_{is} and K_{ii} values determined in the presence of ATP versus AMPPNP are identical, and the K_{is} and K_{ii} values are comparable to one another. Compared to the affinity of the substrate S3 for Lon (K_a = 85 μM, Table 1), the apparent affinities of Pd1 at 500 μM of either nucleotide are 3−4-fold lower (270−300 μM, Table 4).

The steady-state velocities of S3 hydrolysis at varying ATP concentrations against several fixed Pd1 concentrations in the presence of 80 μM or 600 μM of S3 were also determined. The velocity data were best fit by the noncompetitive inhibition eq 3 to yield the respective K_{is} and K_{ii} values as summarized in Table 4. The double reciprocal plots of the peptidase velocities against ATP concentrations in the presence of different concentrations of Pd1 show a series of lines that converge to the left of the ordinate. An exception to the inhibition pattern was noticed in the double reciprocal plot of 600 μM Pd1 against ATP in the presence of 80 or 600 μM of S3 (Figure 5), where the data points either plateau (at 80 μM of S3, Figure 5A) or project upward (at 600 μM of S3, Figure 5B) at saturating ATP. Comparing the K_{is} and K_{ii} values determined for Pd1 at 80 and 600 μM S3 reveals that the inhibitory effect of Pd1 is only affected slightly (2-fold or less) by the 7.5-fold increase of S3 in the reactions (Table 4).

DISCUSSION

Lon is an ATP-dependent protease that functions to eliminate abnormal proteins and to control cellular metabolism by eliminating superfluous enzymes as well as regulatory proteins (*3*). Since enzymes or regulatory proteins are naturally occurring in the cell and their functions are crucial to cell viability, it is important that the degradation of these proteins by Lon is tightly controlled such that cellular homeostasis can be maintained. Because the proteolytic activity of Lon is activated by ATP, but inhibited by the hydrolyzed ATP product ADP (*10*, *21*), the ability to correlate the proteolytic activity of Lon with the dynamic flux of ADP/ATP concentration may provide more insight into the regulatory mechanism of Lon catalysis. Moreover, Lon hydrolyzes polypeptide substrates to yield products that are 5−10 amino acids long; since tetrapeptides, but not the

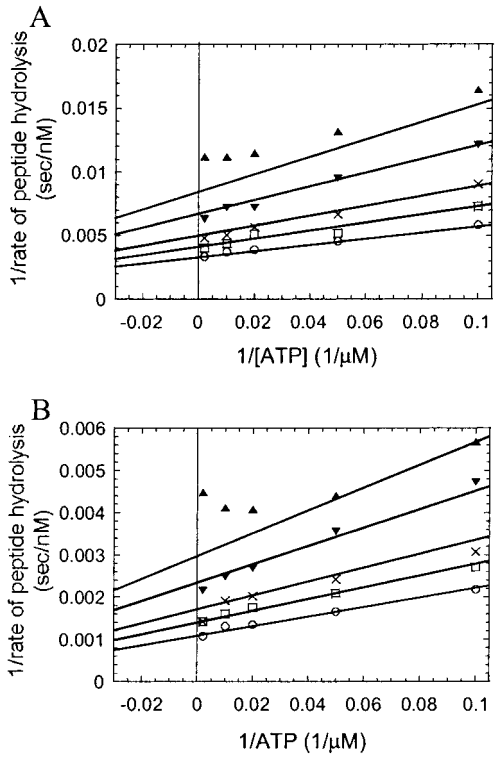

FIGURE 5: Product inhibition of S3 cleavage by Pd1 at varying ATP (10, 20, 50, 100, and 500 μM) in the presence of 80 μM (A) and 600 μM (B) S3. The double reciprocal plots display a series of lines fit from all the experimental data. The symbols represent the averaged data obtained from at least three trials. (A) All assays were performed in the presence of 125 nM *E. coli* Lon monomer and 80 μM S3 at varying ATP and at 0 (○), 100 (□), 200 (×), 400 (▼), and 600 (▲) μM Pd1. (B) All assays were performed in the presence of 125 nM *E. coli* Lon monomer and 600 μM S3 at varying ATP and at 0 (○), 100 (□), 200 (×), 400 (▼), and 600 (▲) μM Pd1.

S1 or S3 peptide substrate, inhibit the ATPase activity of Lon, we question whether the hydrolyzed peptide products of S1 affect the peptidase activity of Lon.

Since S3 contains only one Lon cleavage site and it does not contain any defined secondary structure (*17*), we can directly assess the contribution of ATP hydrolysis toward the peptide cleavage event by comparing the kinetic parameters associated with S3 cleavage accompanied by ATP binding alone or with nucleotide hydrolysis. Assuming that the nonhydrolyzable ATP analogue AMPPNP binding completely mimics the effects of ATP binding in activating the peptidase activity of Lon, we could use AMPPNP to evaluate the kinetic parameters of S3 cleavage resulting from nucleotide binding and ATP to evaluate the kinetic parameters of S3 cleavage resulting from ATP binding and hydrolysis. Figures 3 and 4 and Tables 1 and 2 compare the kinetics of S3 cleavage in the presence of AMPPNP versus ATP. Table 1 shows that the K_b values for the two nucleotides are similar (7.2 μM for ATP and 10 μM for AMPPNP), suggesting that Lon binds either nucleotide with comparable affinity in the presence of S3. In addition, both nucleotide-mediated S3 cleavage reactions yield similar steady-state kinetic parameters with the exception that the k_{cat} of peptide cleavage is 7-fold higher in the presence of ATP versus AMPPNP. The observed difference in the k_{cat} values is consistent with the kinetic data obtained from the pre-steady-state time courses of S3 cleavage at saturating nucleotide concentrations (Table 2). The pre-steady-state kinetic time courses of S3 cleavage display lag kinetics in which the lag rate constant of peptide cleavage at saturating ATP is 6.3-fold higher than that of AMPPNP. Compared to AMPPNP, the v_i and v_f values of ATP-dependent peptide cleavage is 2.5- and 9.3-fold higher, respectively (Table 2). Collectively, our data suggest that ATP affects the k_{cat} of S3 cleavage by accelerating a slow step before the chemical cleavage of peptide bond.

Although the molecular nature of this slow step is currently unknown, this step may represent an ATP-dependent peptide presentation or translocation event prior to substrate cleavage (*2*). This hypothesis is based upon the observation that ATP hydrolysis is used to present or translocate polypeptide substrate to the protease site in other classes of ATP-dependent proteases (*22*−*24*). Since Lon exhibits architectural similarity with these other ATP-dependent proteases (*25*−*27*), it is possible that Lon initially binds ATP and AMPPNP identically but ATP hydrolysis is further used to facilitate the translocation of the S3 substrate to the peptidase site. Because AMPPNP is not hydrolyzed during S3 cleavage, the peptide substrate may gain access to the peptidase site via a passive mechanism. At present, one cannot exclude the possibility that Lon may bind ATP and AMPPNP differently in forming the central complex Lon:nucleotide:S3 prior to peptide cleavage. In this case, the difference in the lag phase in the pre-steady-state time courses of ATP- versus AMPPNP-mediated S3 cleavage would be attributed to the formation of Lon:nucleotide:S3 prior to peptide cleavage instead of a reflection of ATP hydrolysis used to facilitate peptide presentation.

The detection of sigmoidal kinetics in the velocity curves of S3 cleavage suggests cooperativity or allosteric activation of peptide binding. However, it has also been noted that a two-substrate enzyme adopting a steady-state random ordered mechanism with a preferred pathway could display sigmoidal kinetics (*28*, *29*). This could occur if the formation of the Lon:S3 complex and then Lon:S3:nucleotide is kinetically preferred over the formation of Lon:nucleotide followed by Lon:nucleotide:S3. In this model, the rate of peptide hydrolysis is predicted to be inhibited by high nucleotide concentrations at unsaturating levels of S3, a phenomenon that is absent in our study. Therefore the sigmoidal kinetics are likely attributed to cooperativity or allosteric activation by S3.

To further define the kinetic mechanism of ATP-dependent S3 cleavage, we examined the inhibitory effects of ADP on the peptidase activity of Lon as a function of varying either ATP or S3 concentrations. The detection of competitive inhibition in peptide hydrolysis at varying concentrations of ADP against ATP at K_a level of S3 (80 μM) indicates that the two nucleotides compete for the same enzyme form, and that ADP acts as a dead end inhibitor. From the inhibition studies, the intrinsic affinity of ADP (K_{is} and K_{ii}) for Lon in the absence and presence of S3 can be calculated from the relationship $K_{i,apparent} = K_i(1 + [ATP]/K_{ATP})$, where K_i is the apparent K_{is} determined experimentally in Table 3. This result suggests that ADP binds tighter than ATP to free Lon, since the intrinsic K_i of ADP (0.3−0.7 μM) is lower than the K_b of ATP (7.2 μM). Noncompetitive ADP inhibition was detected when S3 was the variable substrate at 10 (1.5 × K_b), 100 (15 × K_b), and 500 μM (70 × K_b) ATP. Comparing the K_{is} values with the K_{ii} values of ADP (Table 3) versus

Scheme 1

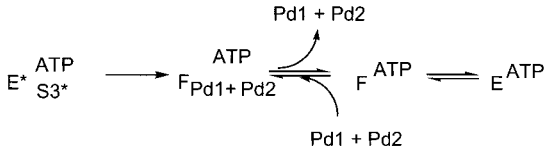

Pd1 and Pd2 are the hydrolyzed peptide products

S3 at the three different ATP levels indicates that the presence of excess S3 weakens the affinity of ADP for Lon by presumably binding allosterically to Lon to promote ATP/ADP exchange in a similar manner as protein substrates. This result distinguishes the S3 peptide substrate from the methoxynaphthylamide tetrapeptides that inhibit the ATPase activity of Lon.

We then utilized the peptide Pd1 as a product inhibitor to study its effect on S3 cleavage with varying ATP as well as with varying S3 concentrations. Noncompetitive inhibition was observed when Pd1 was varied versus S3 at saturating level of ATP or AMPPNP (500 μM). This result suggests that Pd1 binds to two different enzyme forms. Under these reaction conditions, the apparent affinity of S3 for Lon is higher ($K_a = 85$ μM) than the affinity of Pd1 (between 200 and 300 μM), and the K_{is} values are comparable to the K_{ii} values (Table 4), which further suggests that the inhibitory effect of Pd1 cannot be overcome by increasing S3 concentrations. These results can be rectified if Lon isomerizes (an iso-mechanism, *30*) upon S3 cleavage to yield a post catalytic enzyme form that only binds Pd1 but not S3 ("F" in Scheme 1). Because both the ATP and AMPPNP-mediated S3 cleavage reactions exhibited the same inhibition results (Table 4), it is not likely that ATP hydrolysis is associated with Lon isomerization. The molecular nature of the post catalytic Lon form (F) is further revealed by the noncompetitive inhibition patterns obtained when the concentration of Pd1 was varied against ATP at 80 μM as well as at 600 μM S3 (Table 4). According to Figure 5, increasing the ATP concentrations cannot alleviate Pd1 inhibition, and the rates of S3 hydrolysis are further inhibited at high ATP concentrations in the presence of 600 μM Pd1. These observations are consistent with the proposed mechanism in Scheme 1 where the post-catalytic (isomerized) form of Lon binds ATP and Pd1 to form a nonproductive complex that hinders enzyme turnover.

Upon the basis of the results obtained in this study, we have built upon the existing model for Lon catalysis, which assumes that Lon binds ATP and AMPPNP via the same mechanism (*3*) and constructed a kinetic mechanism for the ATP-dependent peptide hydrolysis reaction as shown in Scheme 2. In the absence of S3, Lon (E) hydrolyzes ATP to yield ADP, which binds to Lon more tightly than ATP (steps 1−3). In the presence of S3, we hypothesize that Lon translocates S3 to the peptidase site, accompanied by ATP binding and hydrolysis (steps 1′ and 2′). Since AMPPNP also supports peptide cleavage, it is likely that ATP binding to Lon alone can accomplish peptide translocation, but the rate of this process may be increased by ATP hydrolysis. At saturating S3 and ATP, S3 binds to the allosteric site in Lon to promote ADP/ATP exchange (step 3′−5′). Upon binding of a second molecule of ATP, the translocated peptide (S3*) is hydrolyzed at a specific site to yield small

Scheme 2

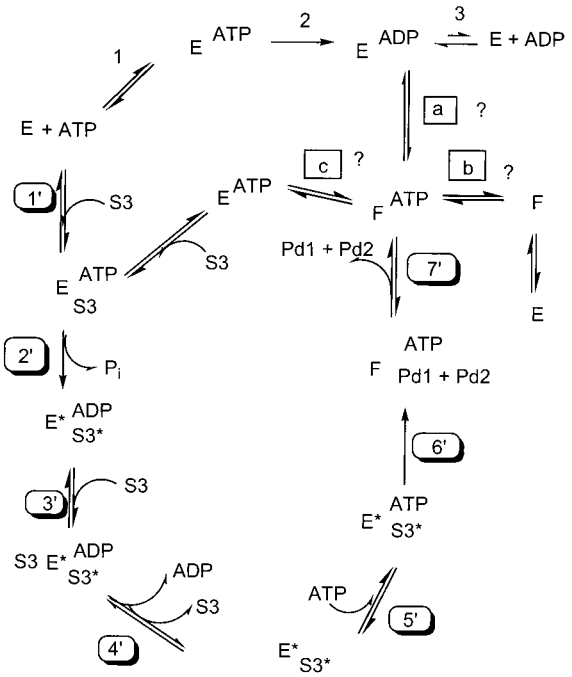

peptide products (Pd1 and Pd2) (step 6′). Consequently, this model predicts that two ATP molecules are used to cleave an amide bond in S3, which is consistent with the detection of two ATP molecules consumed per peptide bond cleavage in protein substrates (*9*). During peptide cleavage, Lon also undergoes an isomerization step to yield a post-catalytic enzyme form (F) that binds ATP and the hydrolyzed peptide products (steps 6′ and 7′). We hypothesize that the conversion of the post catalytic form back to the pre-catalytic form of Lon is required for enzyme turnover although the dynamics of this process have yet to be determined (steps a−c).

It is important to emphasize that the mechanism proposed in Scheme 2 is consistent with the physiological function of a metabolic enzyme, as the proteolytic activity of Lon is regulated by the dynamic flux of ATP, ADP and peptide substrates. Because Lon exhibits ATP-dependent S3 cleavage with concomitant stimulation of ATP hydrolysis, we are currently using pre-steady-state kinetic techniques to elucidate the timing mechanism of ATP binding and hydrolysis with peptide bond cleavage, which should further test the validity of the mechanism proposed in Scheme 2.

ACKNOWLEDGMENT

We wish to thank W. W. Cleland and P. F. Cook for helpful discussion and suggestions made in the preparation of this manuscript.

SUPPORTING INFORMATION AVAILABLE

Experimental procedures and kinetic data for the degradation of S2 peptide, the nonfluorescent analogue of S1, by *E. coli* Lon in the presence of 500 μM ATP. This material is available free of charge via the Internet at http://pubs.acs.org.

REFERENCES

1. Gottesman, S., Gottesman, M. E., Shaw, J. E., and Pearson, M. L. (1981) *J. Cell. Biochem. 32*, 187−191.
2. Maurizi, M. R. (1992) *Experientia 48*, 178−201.

3. Goldberg, A. L., Moerschell, R. P., Chung, C. H., and Maurizi, M. R. (1994) *Methods Enzymol. 244*, 350−75.
4. Charrette, M., Henderson, G. W., and Markovitz, A. (1981) *Proc. Natl. Acad. Sci. U.S.A. 78*, 4728−4732.
5. Suzuki, C. K., Kutejova, E., and Suda, K. (1995) *Methods Enzymol. 260*, 486−94.
6. Wang, N., Maurizi, M. R., Emmert-Buck, L., and Gottesman, M. M. (1994) *J. Biol. Chem. 269*, 29308−13.
7. Wang, N., Gottesman, S., Willingham, M. C., Gottesman, M. M., and Maurizi, M. R. (1993) *Proc. Natl. Acad. Sci. U.S.A. 90*, 11247−51.
8. Van Dyck, L., Pearce, D. A., and Sherman, F. (1994) *J. Biol. Chem. 269*, 238−42.
9. Menon, A. S., Waxman, L., and Goldberg, A. L. (1987) *J. Biol. Chem. 262*, 722−6.
10. Menon, A. S., and Goldberg, A. L (1987) *J. Biol. Chem. 262*, 14929−14934.
11. Van Melderen, L., Thi, M. H. D., Lecchi, P., Gottesman, S., Couturier, M., and Maurizi, M. R. (1996) *J. Biol. Chem. 271*, 27730−8.
12. Maurizi, M. R. (1987) *J. Biol. Chem. 262*, 2696−703.
13. Nishii, W., Maruyama, T., Matsuoka, R., Muramatsu, T., and Takahashi, K. (2002) *Eur. J. Biochem. 269*, 451−7.
14. Waxman, L., and Goldberg, A. L. (1985) *J. Biol. Chem. 260*, 12022−8.
15. Waxman, L., and Goldberg, A. L. (1986) *Science 232*, 500−3.
16. Goldberg, A. L., and Waxman, L. (1985) *J. Biol. Chem. 260*, 12029−34.
17. Lee, I., and Berdis, A. J. (2001) *Anal. Biochem. 291*, 74−83.
18. Wellings, D. A., and Atherton, E. (1997) *Methods Enzymol. 289*, 44−67.
19. Cleland, W. W. (1979) *Methods Enzymol. 63*, 103−38.
20. Frieden, C. (1970) *J. Biol. Chem. 245*, 5788−99.
21. Menon, A. S., and Goldberg, A. L. (1987) *J. Biol. Chem. 262*, 14921−8.
22. Reid, B. G., Fenton, W. A., Horwich, A. L., and Weber-Ban, E. U. (2001) *Proc. Natl. Acad. Sci. U.S.A. 98*, 3768−72.
23. Lee, C., Schwartz, M. P., Prakash, S., Iwakura, M., and Matouschek, A. (2001) *Mol. Cell 7*, 627−37.
24. Ishikawa, T., Beuron, F., Kessel, M., Wickner, S., Maurizi, M. R., and Steven, A. C. (2001) *Proc. Natl. Acad. Sci. U.S.A. 98*, 4328−33.
25. Wang, J., Hartling, J. A., and Flanagan, J. M. (1997) *Cell 91*, 447−56.
26. Sousa, M. C., Trame, C. B., Tsuruta, H., Wilbanks, S. M., Reddy, V. S., and McKay, D. B. (2000) *Cell 103*, 633−43.
27. Stahlberg, H., Kutejova, E., Suda, K., Wolpensinger, B., Lustig, A. Schatz, G., Engel, A., and Suzuki, C. K. (1999) *Proc Natl. Acad. Sci. U.S.A. 96*, 6787−90.
28. Segel, I. H. (1993) *Enzyme Kinetics*, John Wiley and Sons, New York.
29. Copeland, R. A. (1996) *Enzymes. A Practical Introduction to Structure, Mechanism and Data Analysis*, VCH Publisher, New York.
30. Rebholz, K. L. and Northrop, D. B. (1995) *Methods Enzymol. 249*, 211−40.

BI0255470